LA-UR-01-3619
Approved for public release;
distribution is unlimited.

Title: **Recent results from the microscopic Schrödinger optical model**

Author(s): S. Karataglidis

Submitted to:

http://lib-www.lanl.gov/la-pubs/00796312.pdf

Recent results from the microscopic Schrödinger optical model

S. Karataglidis

LANL

Collaborators:

K. Amos, P. K. Deb (Melbourne),

B. A. Brown (NSCL/MSU),

D. G. Madland, M. B. Chadwick (LANL),

Outline

- Motivation.
- Formal theory of the OMP.
- NN g matrices.
- Effective NA interaction and optical potential.
- Nuclear structure
- Results:
  - Neutron scattering: ^{12}C, ^{40}Ca, ^{56}Fe, and ^{208}Pb.
  - Integral observables: ^{12}C and ^{208}Pb.
  - Comparison with Dirac phenomenology: ^{208}Pb.
  - Exotic nuclei: ^{6}He, ^{10}C and ^{11}Be.
- Conclusions.

Motivation

Why a microscopic description of nucleon-nucleus (NA) scattering?

- Direct probe of the matter density, complementary to electron scattering probing the charge and current densities.
- A “parameter-free” description.
- For $A = 1$, should recover NN scattering.
- Interest in detailed optical potentials in many fields: structure, exotic nuclei, astrophysics, ($e, e'N$), medical physics, etc.

Review: K. Amos, P. J. Dortmans, H. V. von Geramb, S. K., and J. Raynal, Adv. Nucl. Phys. **25**, 275 (2000).

Formal theory of the NA optical potential

Consider the elastic channel and associate the term optical potential only with this channel. Using projections operators, divide the Hilbert space into two:

- P projecting onto the elastic channel.
- Q projects onto everything else.

$$(E - H_{PP}) \left|\Psi^+\right\rangle = H_{PQ} \left|\Psi^+\right\rangle$$
$$(E - H_{QQ}) \left|\Psi^+\right\rangle = H_{QP} \left|\Psi^+\right\rangle$$

and

$$\left(E - H_{PP} - H_{PQ} \left[E - H_{QQ} + i\varepsilon\right]^{-1} H_{QP}\right) \left|\Psi^+\right\rangle = 0$$

Reducing to an effective one-body problem:

$$\left(E - H_0 - \left\langle \Phi_{gs} \right| V \left| \Phi_{gs} \right\rangle - \left\langle \Phi_{gs} \left| V G^{(+)}_{QQ} V \right| \Phi_{gs} \right\rangle\right) \left|\chi^+\right\rangle = 0,$$

where $G^{(+)}_{QQ} = \left[E - H_{QQ} + i\varepsilon\right]^{-1}$.

The optical potential is identified by:

$$U = U_{\text{OM}}(E) = \langle \Phi_{gs} | V | \Phi_{gs} \rangle + \left\langle \Phi_{gs} \left| V G^{(+)}_{QQ} V \right| \Phi_{gs} \right\rangle .$$

It is a many body problem.

Properties:

- It is non-local and complex.
- Energy-dependent from the second term.
- Multiple scattering coming from presence of the second term.

t or g ..... ?

Using the t matrix in the optical potential neglects medium effects (density, Pauli blocking). Start, instead, with the nuclear matter g matrix in infinite matter.

Solution of the Bruckner-Bethe-Goldstone equation:

$$g^{(JST)}(\boldsymbol{q}', \boldsymbol{q}; \boldsymbol{K}) = V^{(JST)}(\boldsymbol{q}', \boldsymbol{q}) + \int V^{(JST)}(\boldsymbol{q}', \boldsymbol{k}') \frac{Q(\boldsymbol{k}', \boldsymbol{K}; k_f)}{E(\boldsymbol{k}, \boldsymbol{K}) - E(\boldsymbol{k}', \boldsymbol{K}) - i\varepsilon} g^{(JST)}(\boldsymbol{k}', \boldsymbol{q}; \boldsymbol{K})\, d\boldsymbol{k}'$$

Initial momenta denoted by $\boldsymbol{p}_0$ (projectile) and $\boldsymbol{p}_1$ (bound state nucleon). $\boldsymbol{k}, \boldsymbol{K}$ are relative and C.M. momenta. Primes denote final state, k_f is the Fermi momentum. Q is an angle-averaged Pauli operator, and the energy denominator contains mass-dependent terms.

In practical calculations at intermediate energies use angle averages as good approximations.

Coordinate space representation

Map:

$$g^{(JST)}\left(\boldsymbol{p}', \boldsymbol{p}; E, k_f\right) \rightarrow g^{(JST)}\left(\boldsymbol{r}, E, \rho\left\{k_f(r)\right\}\right),$$

where $\boldsymbol{r} \rightarrow \left|\boldsymbol{r}_0 - \boldsymbol{r}_1\right| = r$.

Definition: mapping to operator forms, effective g matrices.....

$$g_{\text{eff}}^{(JST)}(\boldsymbol{r}, E; k_f) = \sum_i g_{\text{eff}}^{(i)(JST)}(r, E; k_f)\Theta_i$$

where $g_{\text{eff}}^{(i)(JST)}(r, E; k_f) = \sum_{j=1}^{n_i} S_j^{(i)}(E; k_f)\frac{e^{-\mu_j^{(i)} r}}{r}$,

- Θ_i — characteristic operators:
  - $i = 1$: central forces: $\{1, (\sigma \cdot \sigma), (\tau \cdot \tau), (\sigma \cdot \sigma\tau \cdot \tau)\}$
  - $i = 2$: tensor force: $\{S_{12}\}$
  - $i = 3$: two-body spin-orbit force: $\{\boldsymbol{L} \cdot \boldsymbol{S}\}$
- $S_j^{(i)}(E; k_f)$ — complex, energy-dependent strengths.

Construction of the OMP

Formally, in coordinate space, the OMP for elastic scattering is:

$$U(\boldsymbol{r},\boldsymbol{r}';E) = \delta(\boldsymbol{r}-\boldsymbol{r}')\sum_i n_i \int \varphi_i^*(\boldsymbol{s}) g_D(\boldsymbol{r},\boldsymbol{s};E)\varphi_i(\boldsymbol{s})\,d\boldsymbol{s}$$

$$+\sum_i n_i\,\varphi_i^*(\boldsymbol{r})\,g_E(\boldsymbol{r},\boldsymbol{r}';E)\,\varphi_i(\boldsymbol{r}')$$

$$= U_D(\boldsymbol{r};E)\,\delta(\boldsymbol{r}-\boldsymbol{r}') + U_E(\boldsymbol{r},\boldsymbol{r}';E)\ ,$$

D, E denote direct and exchange contributions, respectively. n_i are the occupation numbers of the ground state.

First term contains the "$t\rho$" or "$g\rho$" contributions to the optical potential. The nonlocality arises purely out of the exchange terms. For $J \neq 0$ targets, terms with $I \neq 0$ may be included in the DWA.

Integral observables

The S matrix defines the phase shifts $\delta_l^{\pm}(k)$

$$S_l^{\pm} \equiv S_l^{\pm}(k) \quad = \quad e^{2i\delta_l^{\pm}(k)} = \eta_l^{\pm}(k) e^{2i\Re\left[\delta_l^{\pm}(k)\right]}$$

With $E \propto k^2$,

$$\begin{aligned}
\sigma_{\text{el}}(E) &= \frac{\pi}{k^2} \sum_{l=0}^{\infty} \left\{ (l+1) \left| S_l^{+} - 1 \right|^2 + l \left| S_l^{-} - 1 \right|^2 \right\} , \\
\sigma_R(E) &= \frac{\pi}{k^2} \sum_{l=0}^{\infty} \left\{ (l+1) \left[1 - \left(\eta_l^{+}\right)^2 \right] + l \left[1 - \left(\eta_l^{-}\right)^2 \right] \right\} , \\
\sigma_{\text{TOT}}(E) &= \sigma_{\text{el}}(E) + \sigma_R(E)
\end{aligned}$$

Specification of target: nuclear structure

The shell model is utilised. One-body density matrix elements (OBDME)

$$S_{j_1 j_2 J} = \left\langle J_f \left\| \left[a^\dagger_{j_2} \times \tilde{a}_{j_1} \right]^J \right\| J_i \right\rangle$$

Models used:

$A \leq 16$ Multi-$\hbar\omega$ models in *no-core* calculations. All core polarisations (to level of $\hbar\omega$) explicitly included. Interactions used: MK3W (Millener-Kurath based), WBT (Warburton and Brown).

$16 < A \leq 40$ $0\hbar\omega$ models using USD interaction of Wildenthal and Brown. PHF model also used in case of rotational bands.

$A > 40$ Restricted $0\hbar\omega$ in the lower fp-shell; simple packed orbits for everything else (elastic scattering only). For ^{208}Pb, Skyrme-Hartree-Fock model of Brown [PRL **85**, 5296 (2000)].

Where possible, electron scattering is used to test the model and also specify the single particle wave functions.

Phenomenological Dirac model

[R. Kozack and D. G. Madland, Phys. Rev. C **39**, 1461 (1989).]

- Potential specified by spherically symmetric Lorentz isoscalar-scalar and isoscalar-vector potentials together with Coulomb interaction in a Walecka-like model.
- Second-order reduction of Dirac equation leads to a Schrödinger equivalent equation, with physically correct effective central and spin-orbit potentials, plus the Coulomb correction term.
- Projectile and target isospin treated by introducing corresponding isovector potentials in relativistic Lane model.
- Fitting of complete data set for ^{208}Pb determines parameter set.

Results

Neutron scattering Comparison of proton and neutron scattering from ^{12}C, ^{40}Ca, ^{56}Fe, and ^{208}Pb.

Integral observables Total reaction and total cross sections for scattering from ^{12}C and ^{208}Pb.

Comparison of models Comparing results of Dirac phenomenology with microscopic Schrödinger for nucleon scattering from ^{208}Pb.

Exotic nuclei Recent results for ^{6}He, ^{11}Be and ^{10}C.

In what follows: MOMP = Microscopic optical model potential; POMP = Phenomenological optical model potential.

Neutron scattering

^{12}C:

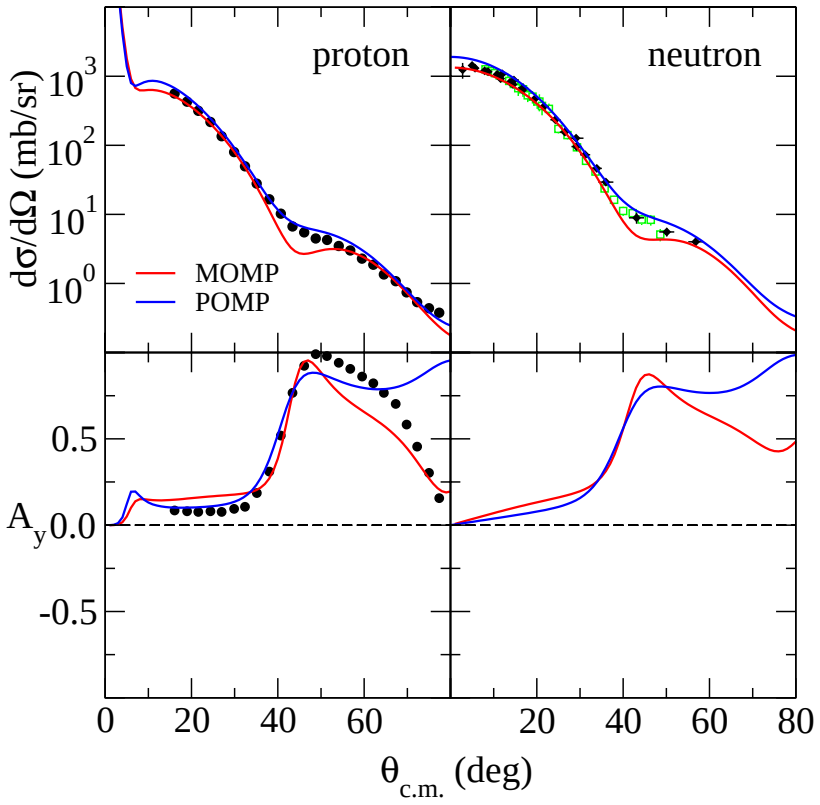

Figure 1: Differential cross sections and analyzing power for 65 MeV proton and neutron elastic scattering from ^{12}C.

$\sigma_{\rm el}({\rm b}) = 0.417({\rm M});\ 0.559({\rm P})$

$\sigma_{\rm R}({\rm b}) = 0.331({\rm M});\ 0.270({\rm P})$

$\sigma_{\rm TOT}({\rm b}) = 0.748({\rm M});\ 0.829({\rm P});\ 0.753 \pm 0.005$

^{56}Fe:

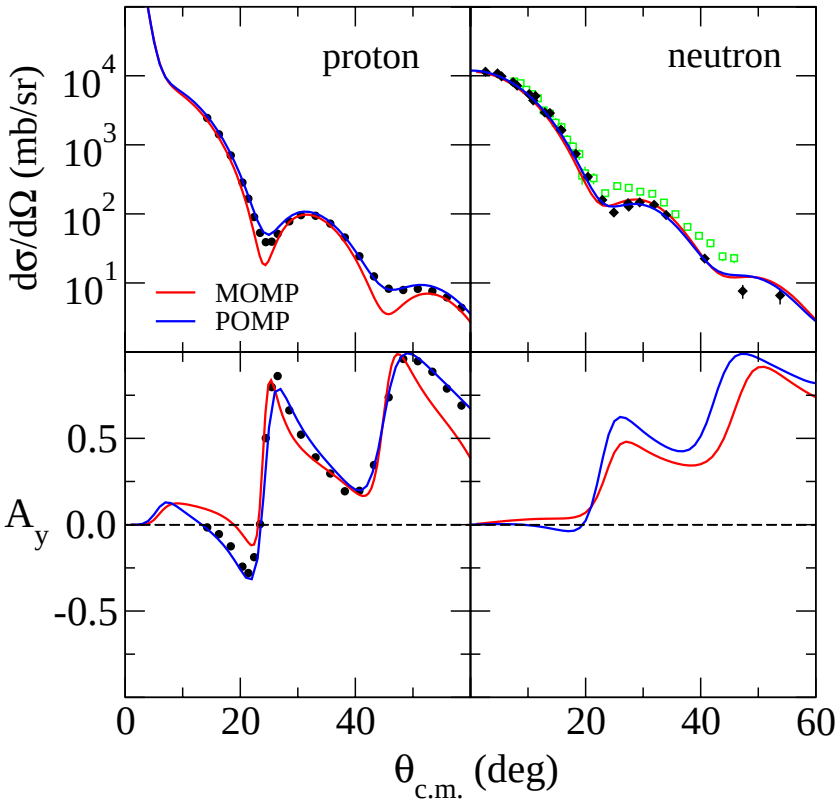

Figure 2: As for Fig. 1, but for ^{56}Fe.

$\sigma_{\rm el}({\rm b}) = 1.370({\rm M});\ 1.456({\rm P})$

$\sigma_{\rm R}({\rm b}) = 0.964({\rm M});\ 0.885({\rm P})$

$\sigma_{\rm TOT}({\rm b}) = 2.334({\rm M});\ 2.341({\rm P});\ 2.40 \pm 0.01$

^{40}Ca:

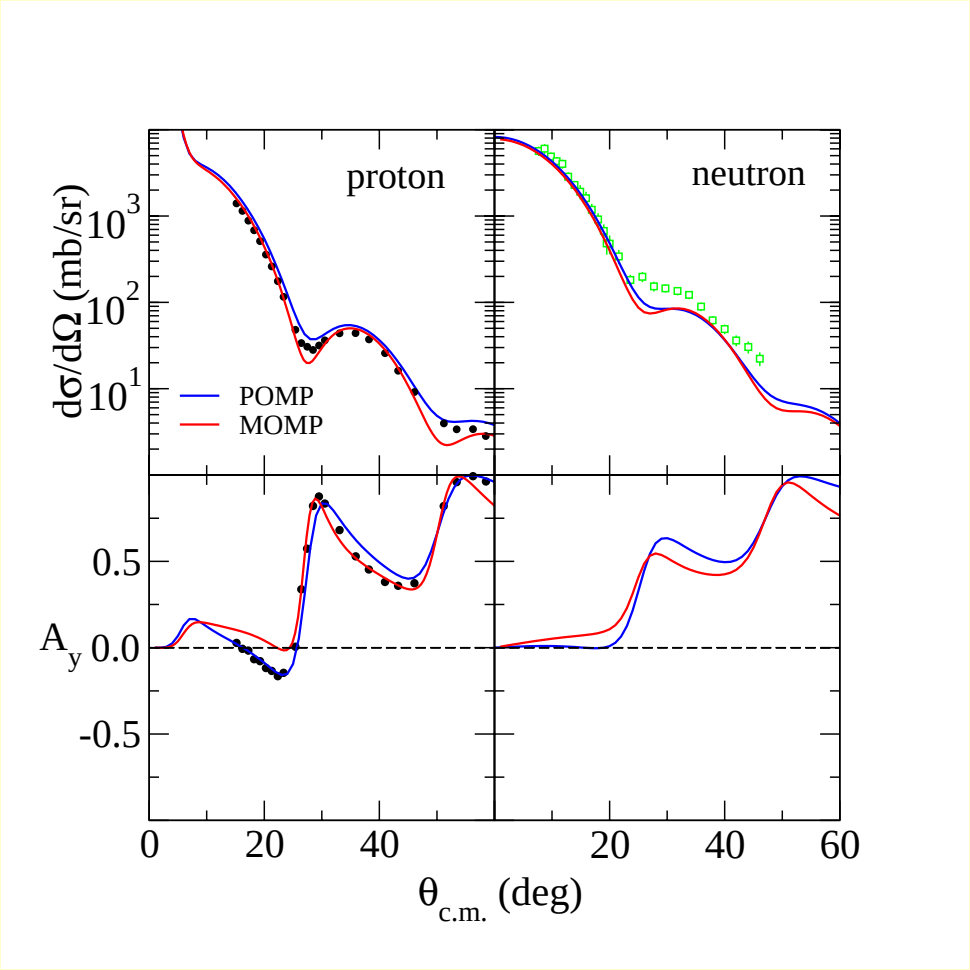

Figure 3: As for Fig. 1, but for ^{40}Ca.

$\sigma_{\rm el}({\rm b}) = 1.122({\rm M});\ 1.220({\rm P})$

$\sigma_{\rm R}({\rm b}) = 0.788({\rm M});\ 0.684({\rm P})$

$\sigma_{\rm TOT}({\rm b}) = 1.910({\rm M});\ 1.904({\rm P});\ 1.966 \pm 0.009$

Can one deduce the neutron density in ^{208}Pb?

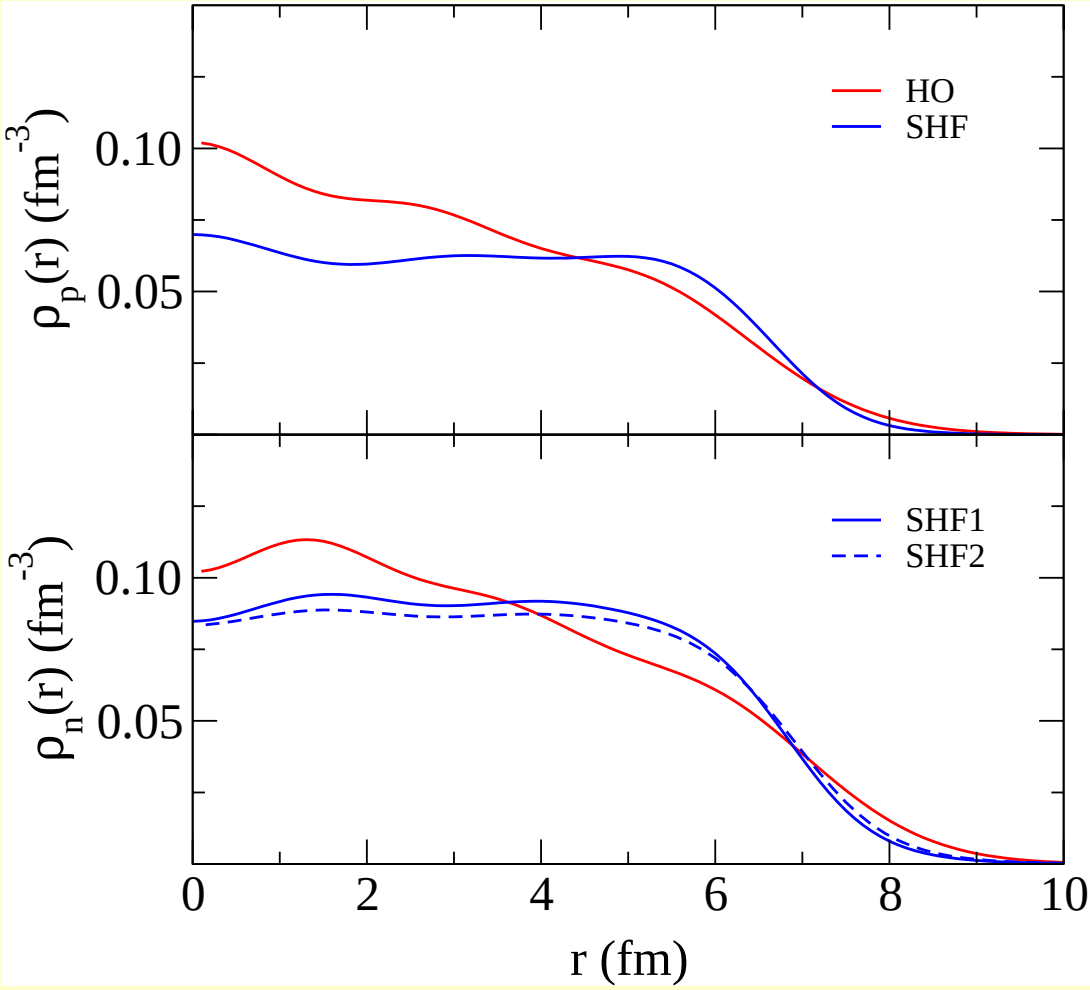

Figure 4: Proton and neutron densities for ^{208}Pb.

Table 1: Root-mean-square radii for ^{208}Pb from the SHF and $0\hbar\omega$ HO models.

Model	r_p (fm)	r_n (fm)	$r_n - r_p$ (fm)
$0\hbar\omega$ I	5.45	5.83	0.38
$0\hbar\omega$ II	5.45	5.60	0.15
SHF1	5.45	5.60	0.15
SHF2	5.45	5.70	0.25

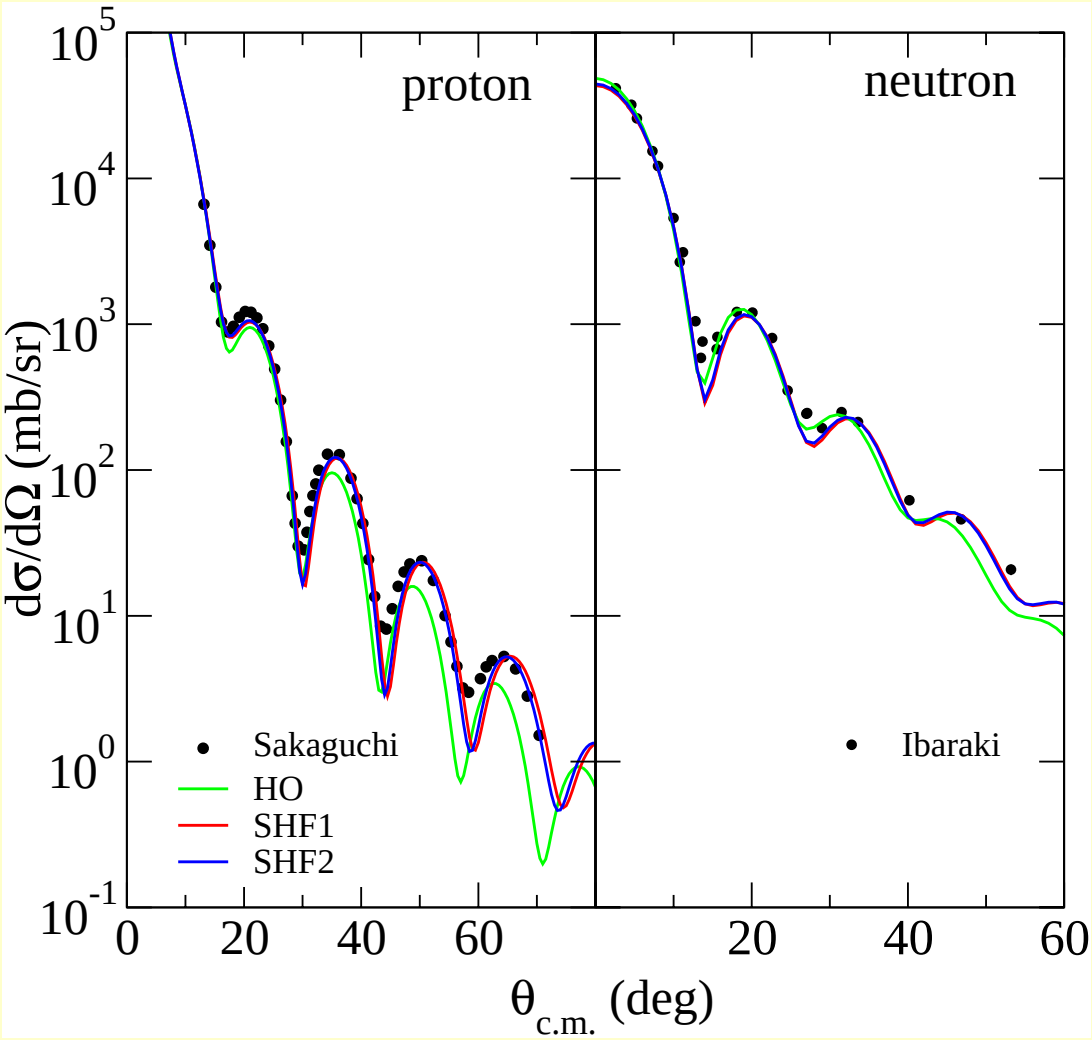

Figure 5: Differential cross section for elastic scattering of 65 MeV protons and neutrons from ^{208}Pb.

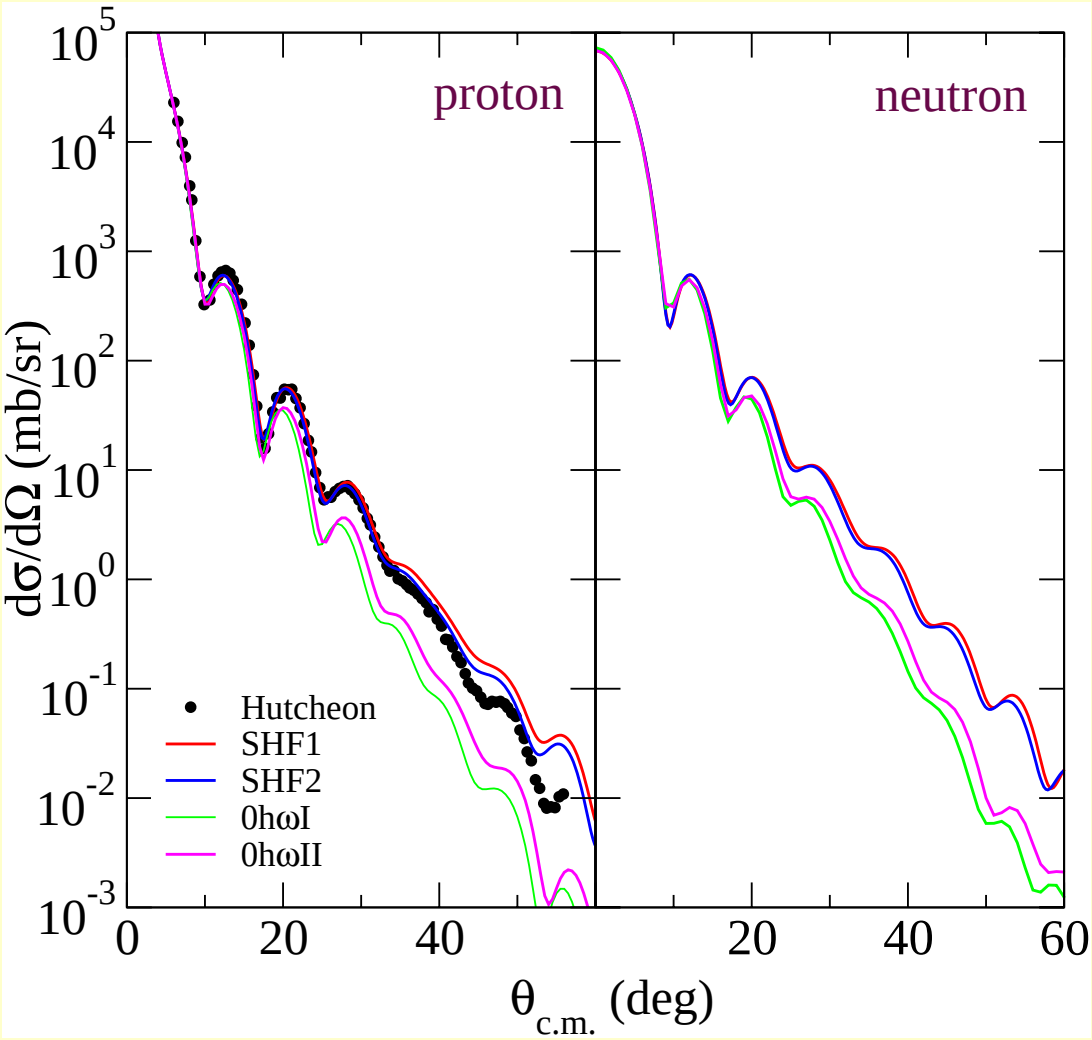

Figure 6: Differential cross section for elastic scattering of 200 MeV protons and neutrons from ^{208}Pb.

Comparison of Dirac phenomenology and microscopic Schrödinger

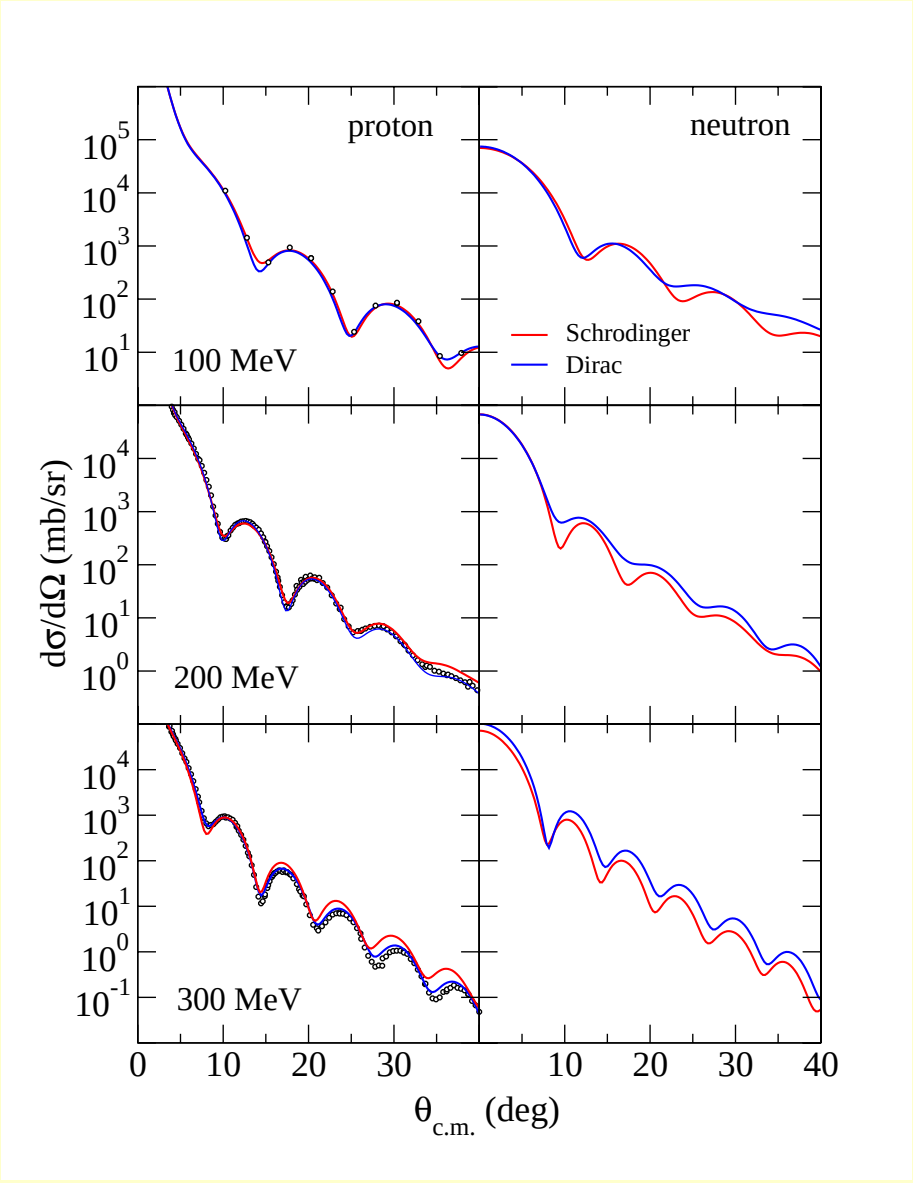

Figure 7: Differential cross sections for N-^{208}Pb elastic scattering.

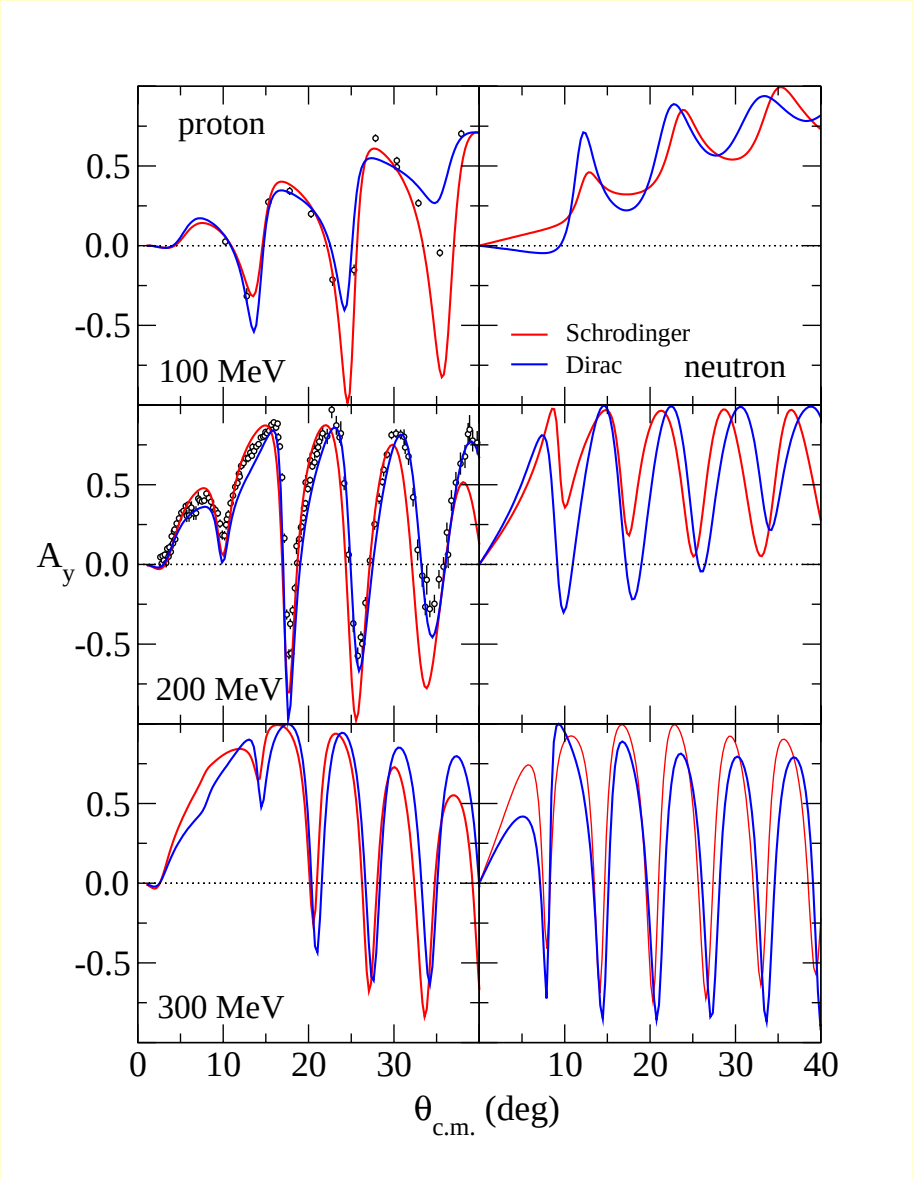

Figure 8: Analyzing powers for N-^{208}Pb elastic scattering.

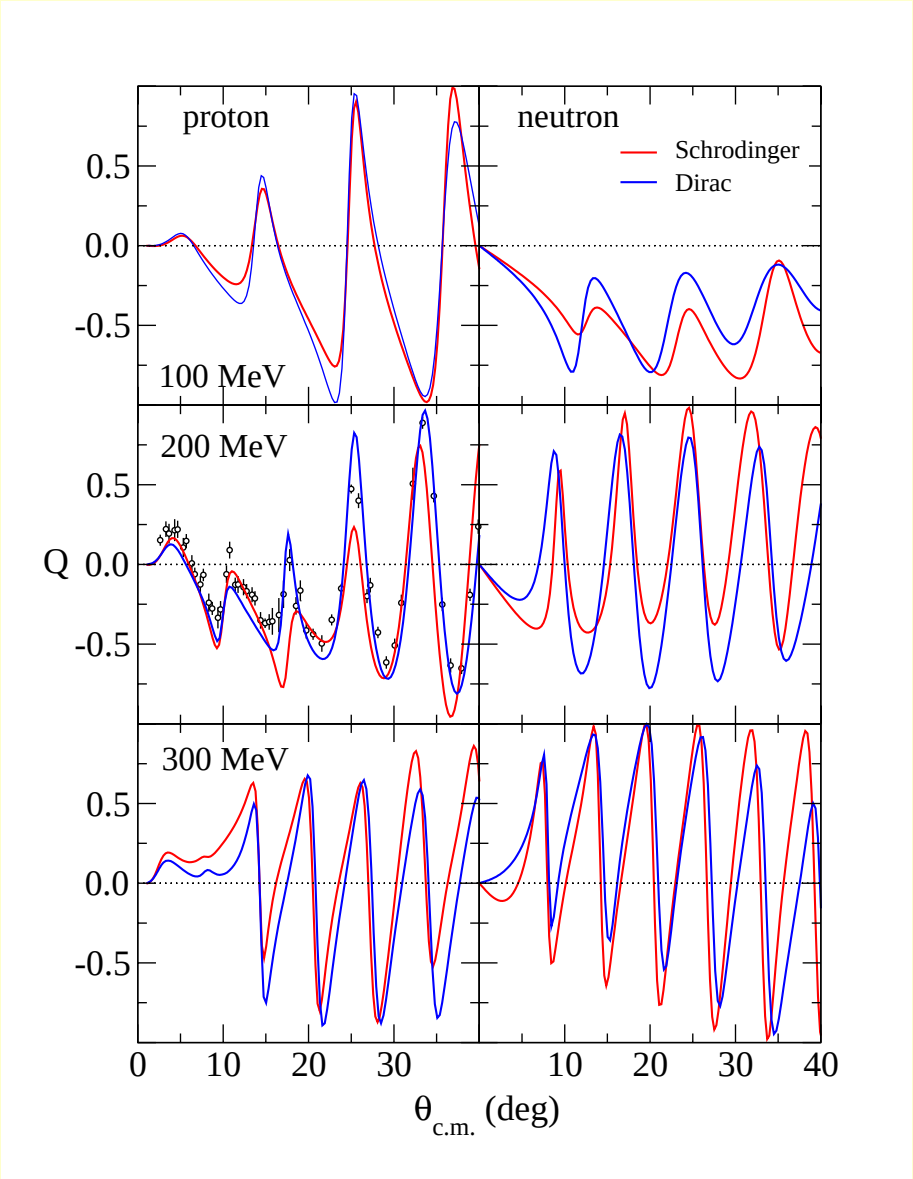

Figure 9: Spin rotations for N-^{208}Pb elastic scattering.

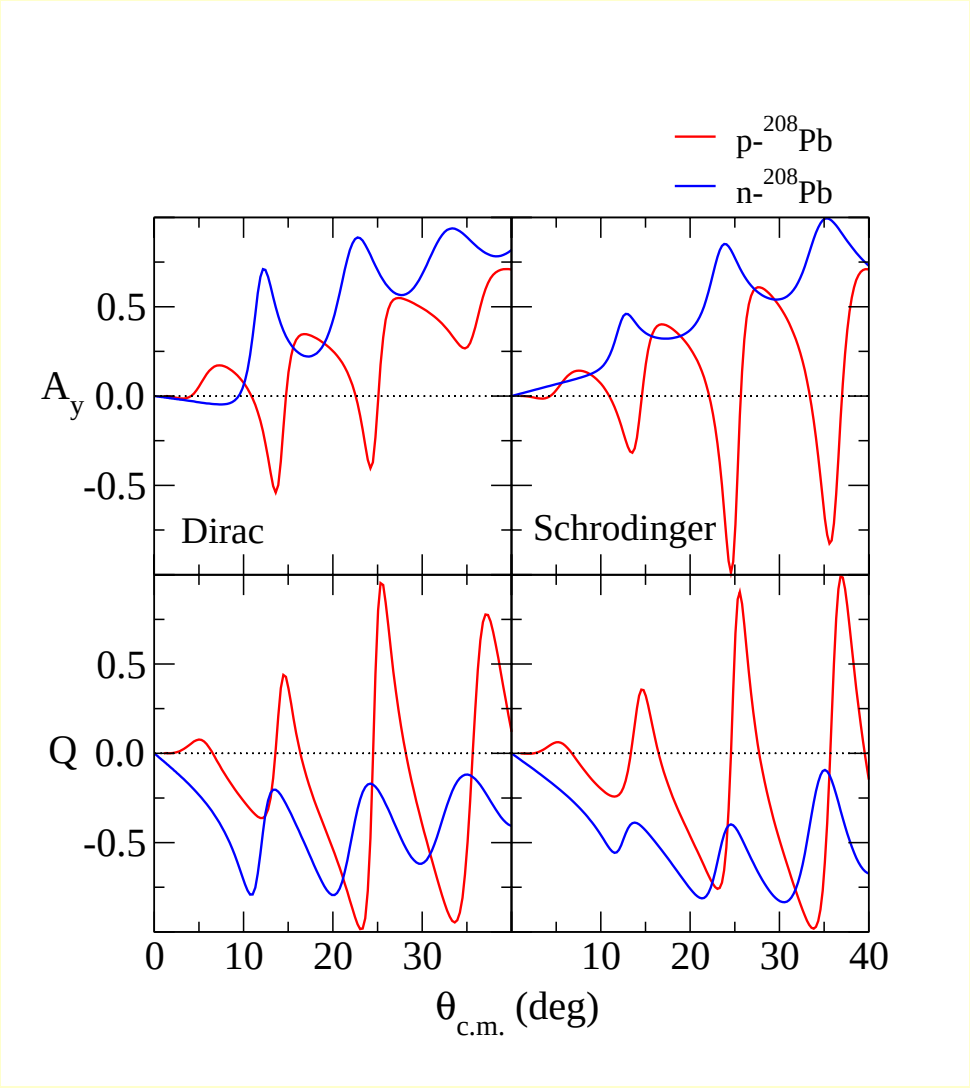

Figure 10: Spin observables for 100 MeV N-^{208}Pb elastic scattering.

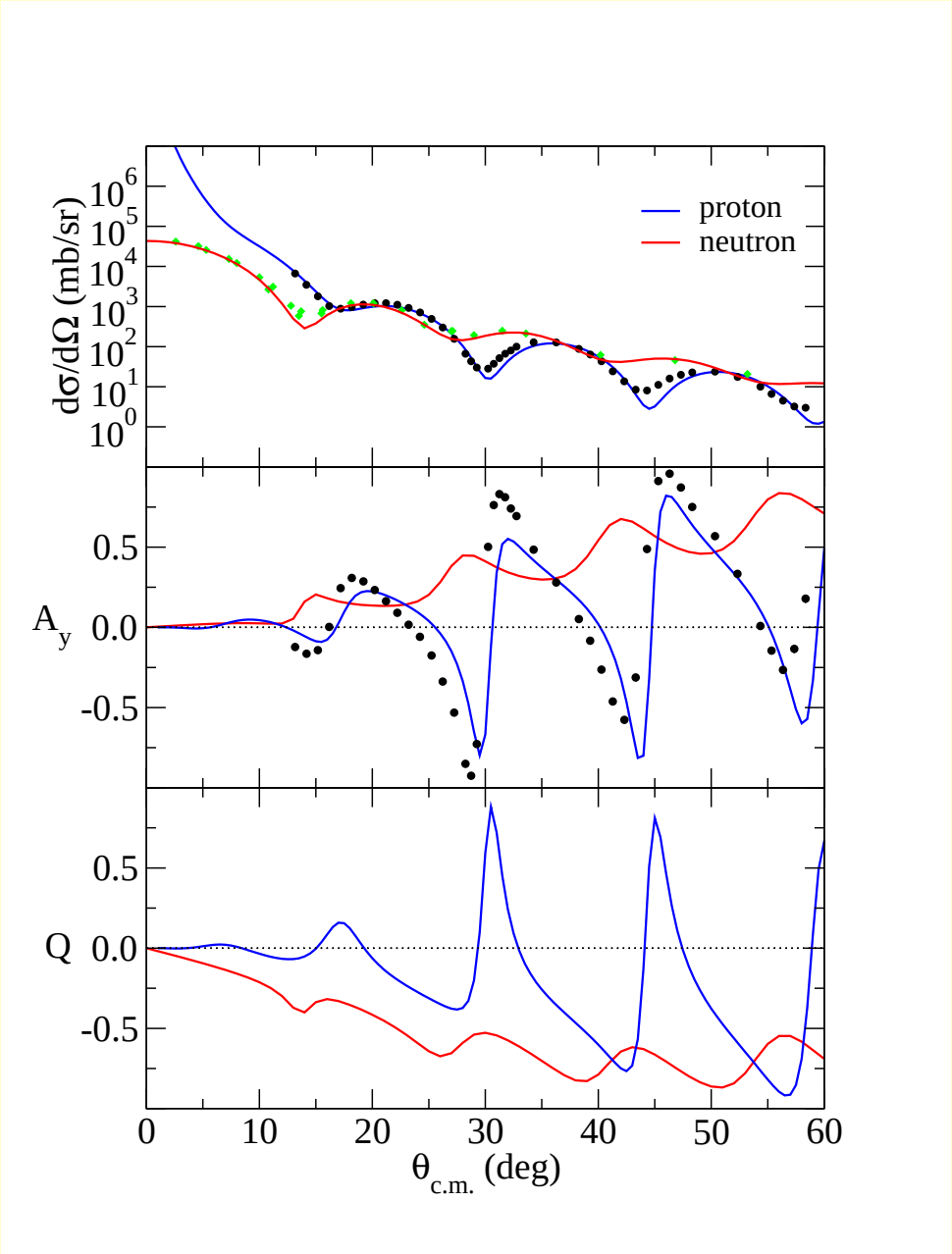

Figure 11: Observables for 65 MeV N-^{208}Pb elastic scattering.

Integral observables

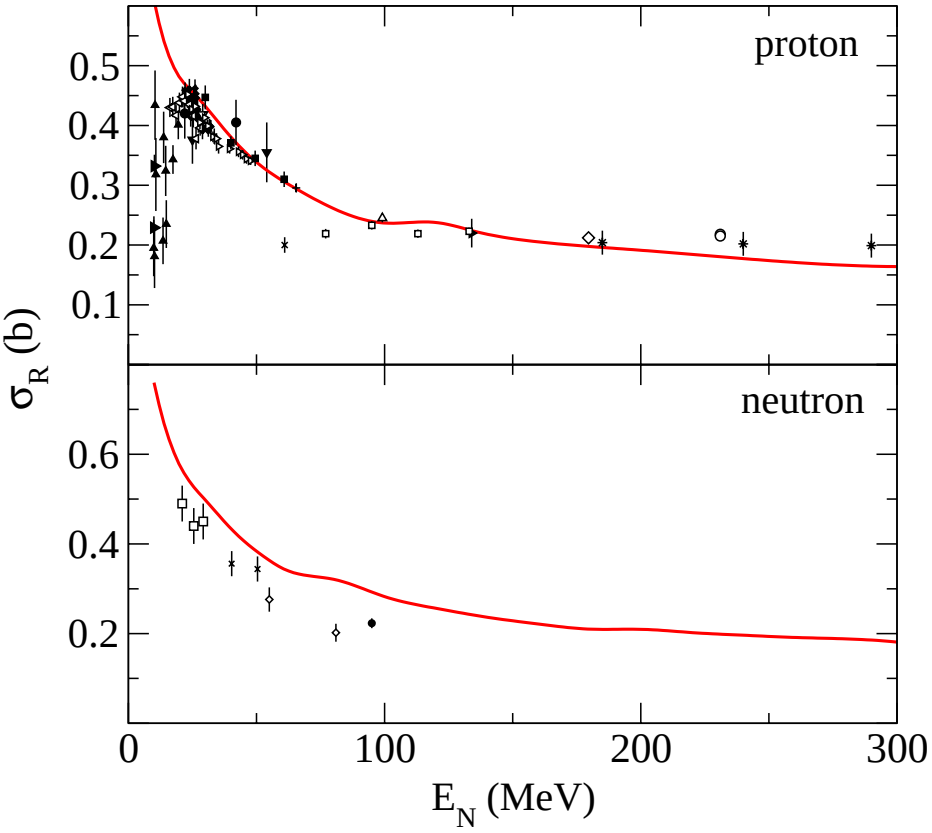

Figure 12: Total reaction cross section for proton and neutron scattering from ^{12}C.

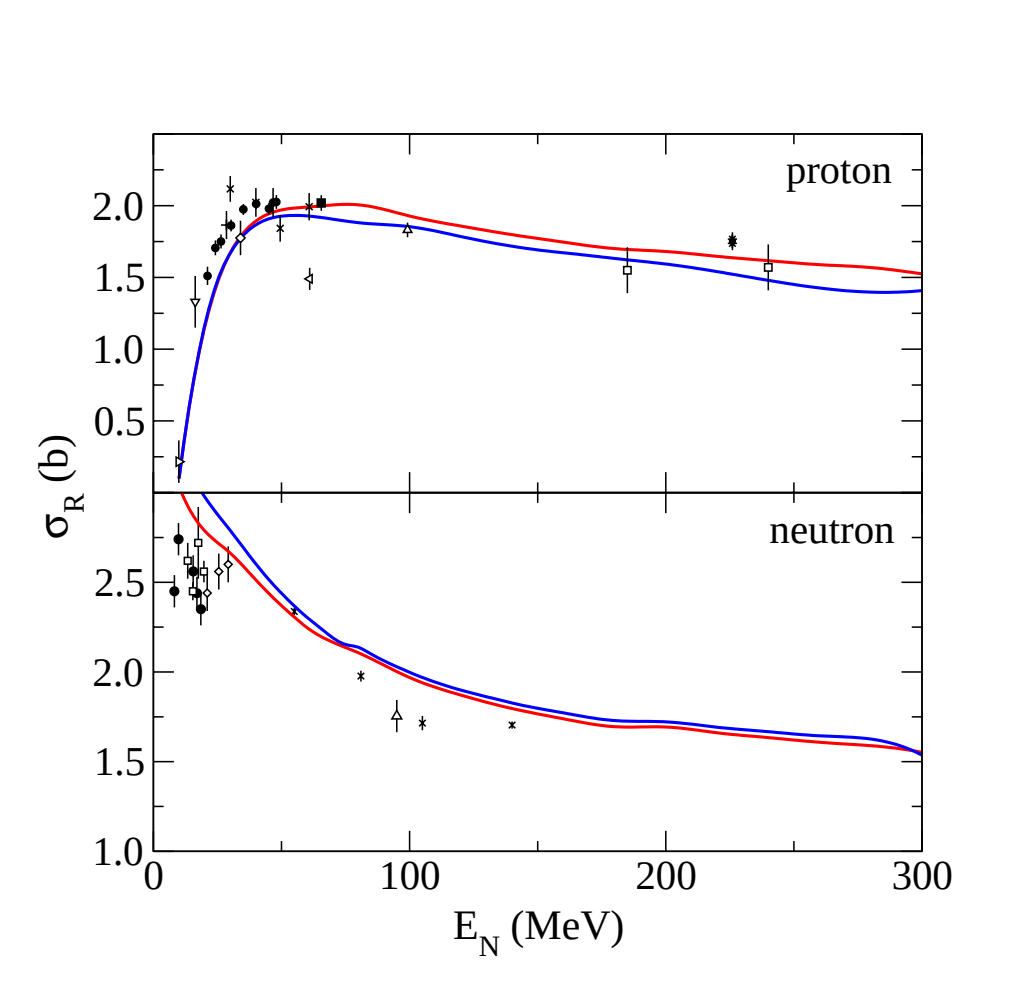

Figure 13: Total reaction cross section for proton and neutron scattering from ^{208}Pb.

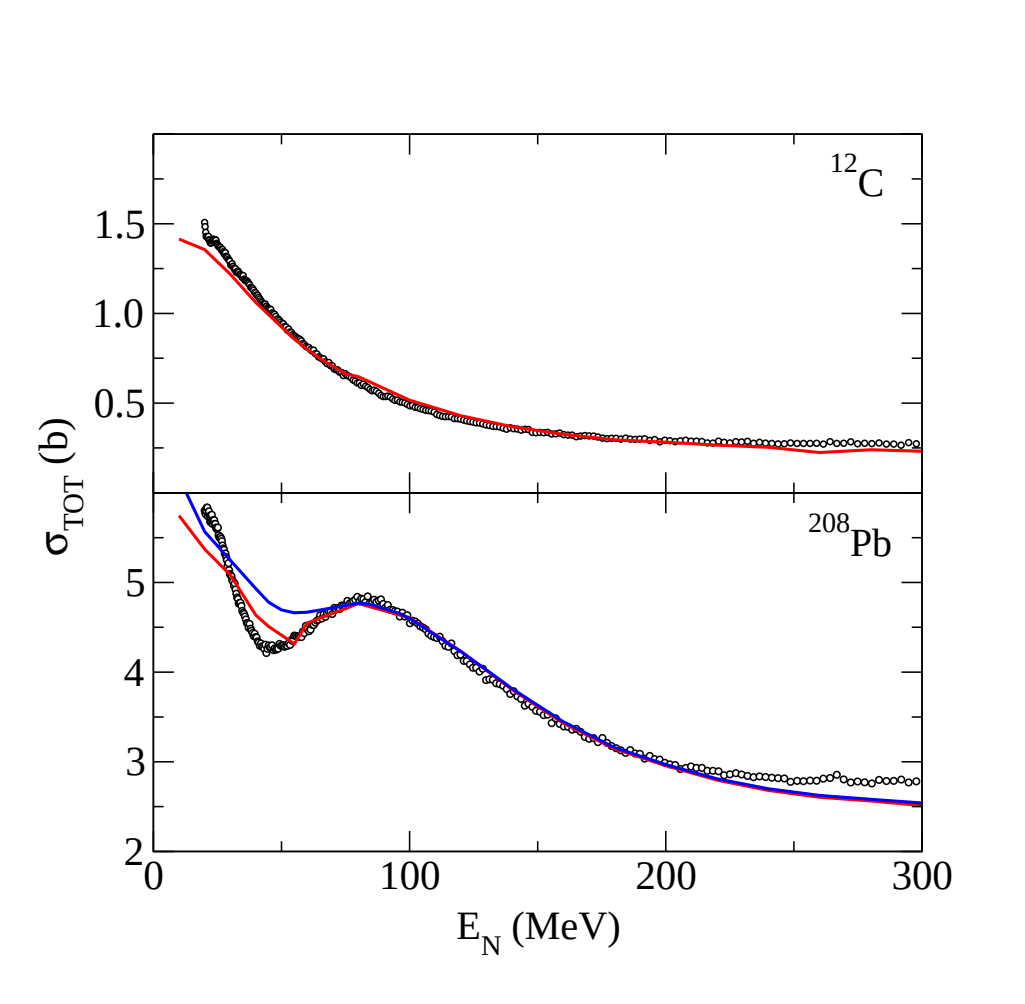

Figure 14: Total neutron scattering cross sections from ^{12}C and ^{208}Pb.

Exotic nuclei: ^{6}He

$4\hbar\omega$ shell model calculation using interaction of Zheng *et al.*

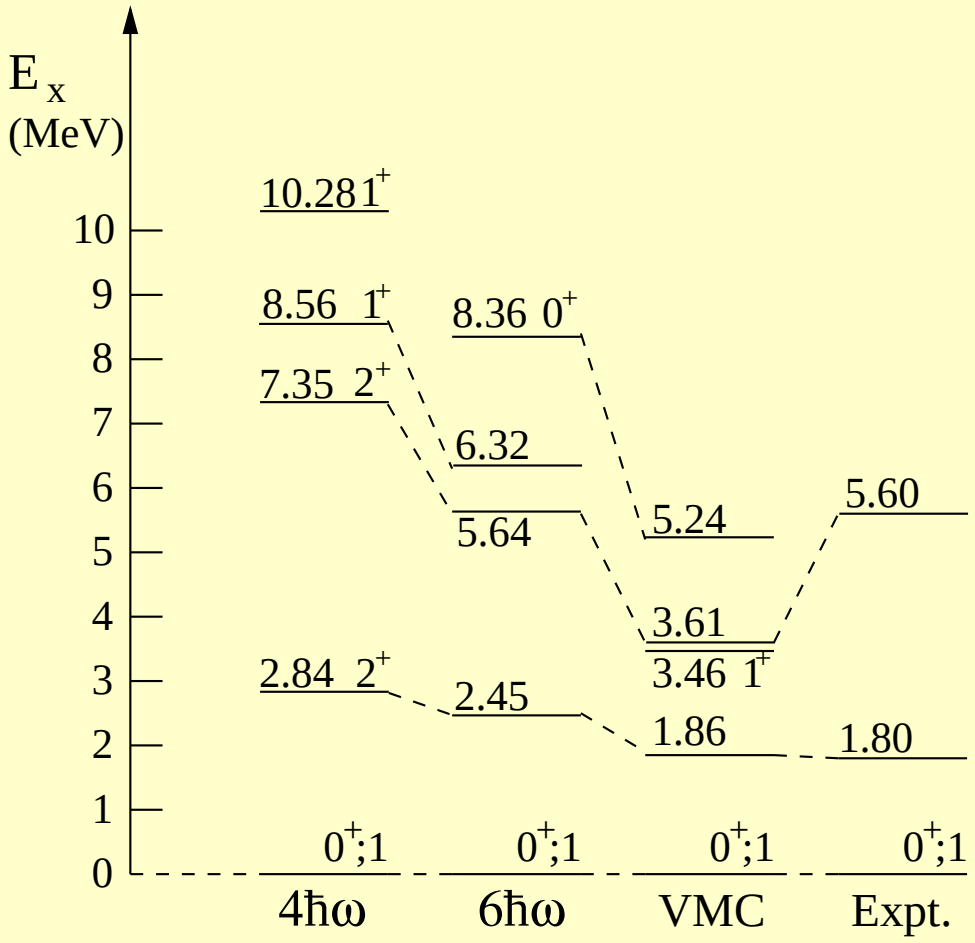

Figure 15: Spectrum of ^{6}He.

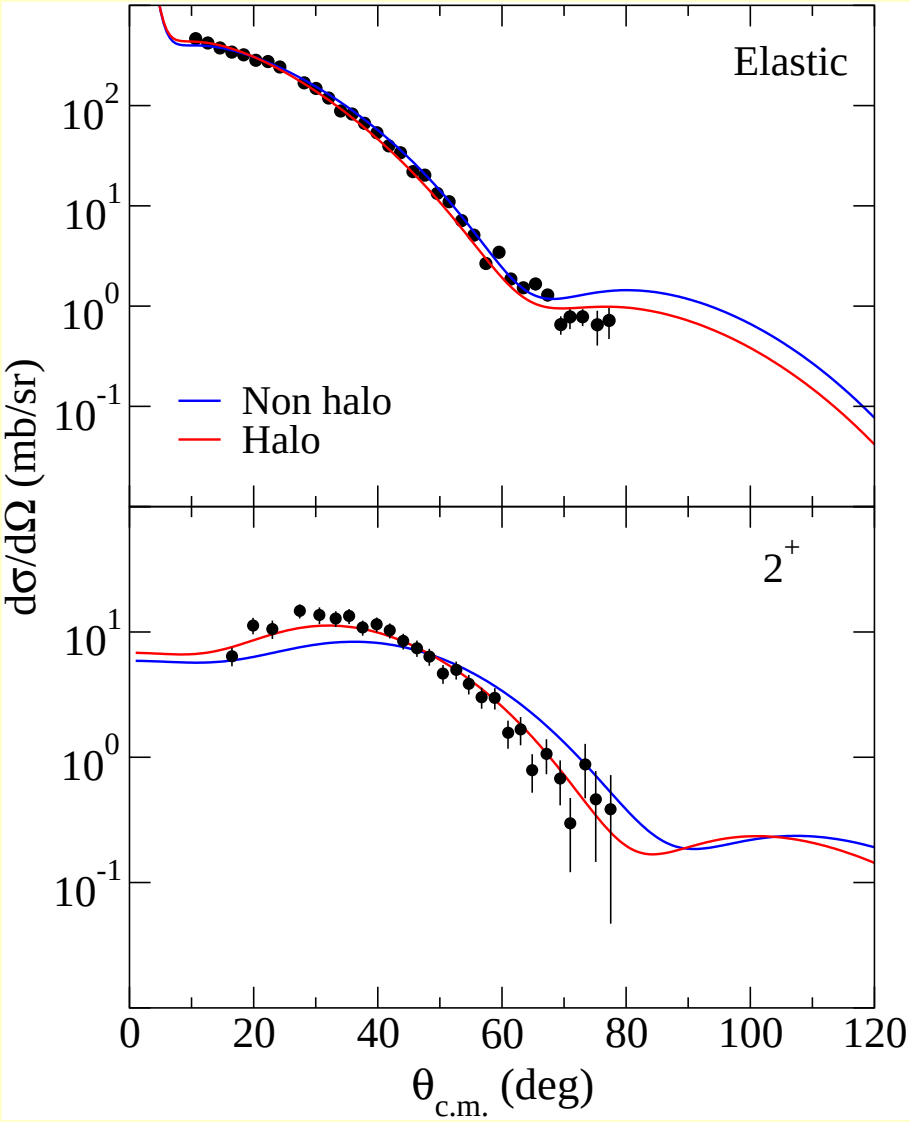

Figure 16: Differential cross sections for elastic and inelastic scattering of protons from ^{6}He. $\sigma_r = 353$ mb (nonhalo), 406 mb (halo), 410 ± 21 mb (expt)

^{11}Be$(p,n)^{11}$B(IAS)

Complete (0+2)$\hbar\omega$ shell model using WBT interaction.

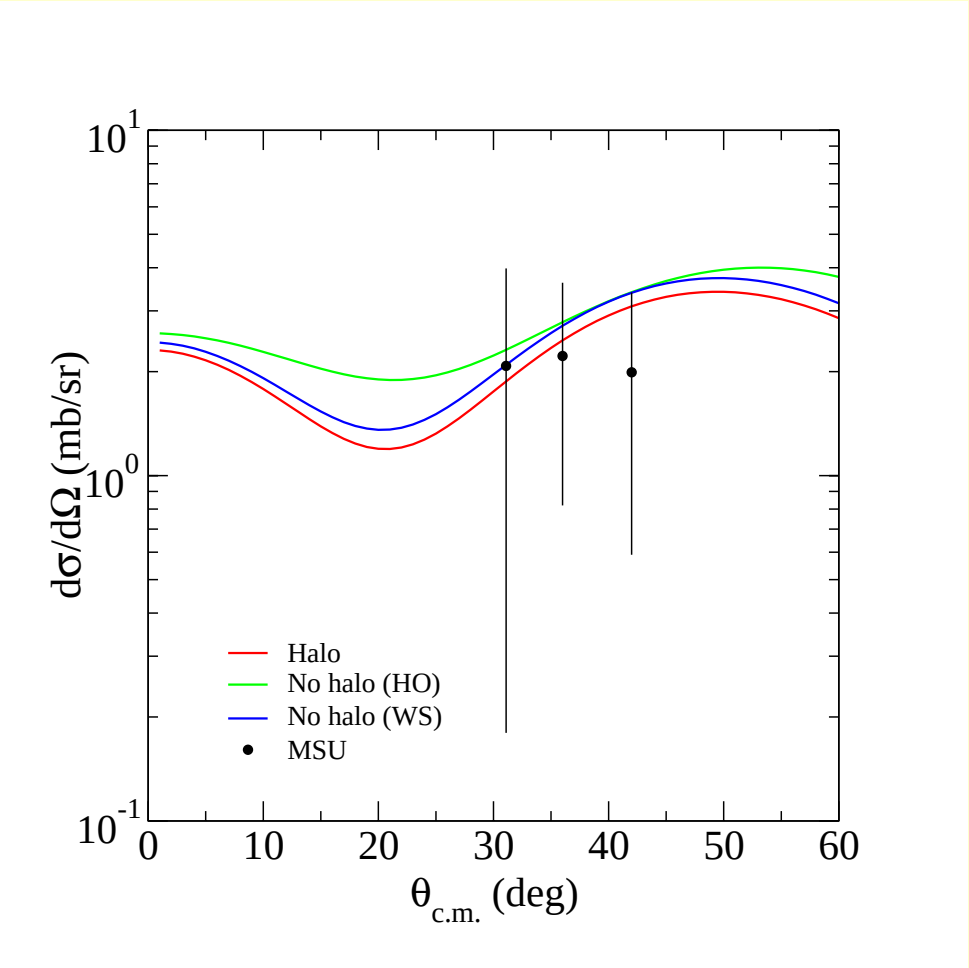

Figure 17: ^{11}Be$(p,n)^{11}$B(IAS) differential cross section at 30 MeV.

^{10}C elastic and inelastic scattering

Complete (0+2)$\hbar\omega$ shell model using MK3W and WBT interactions.

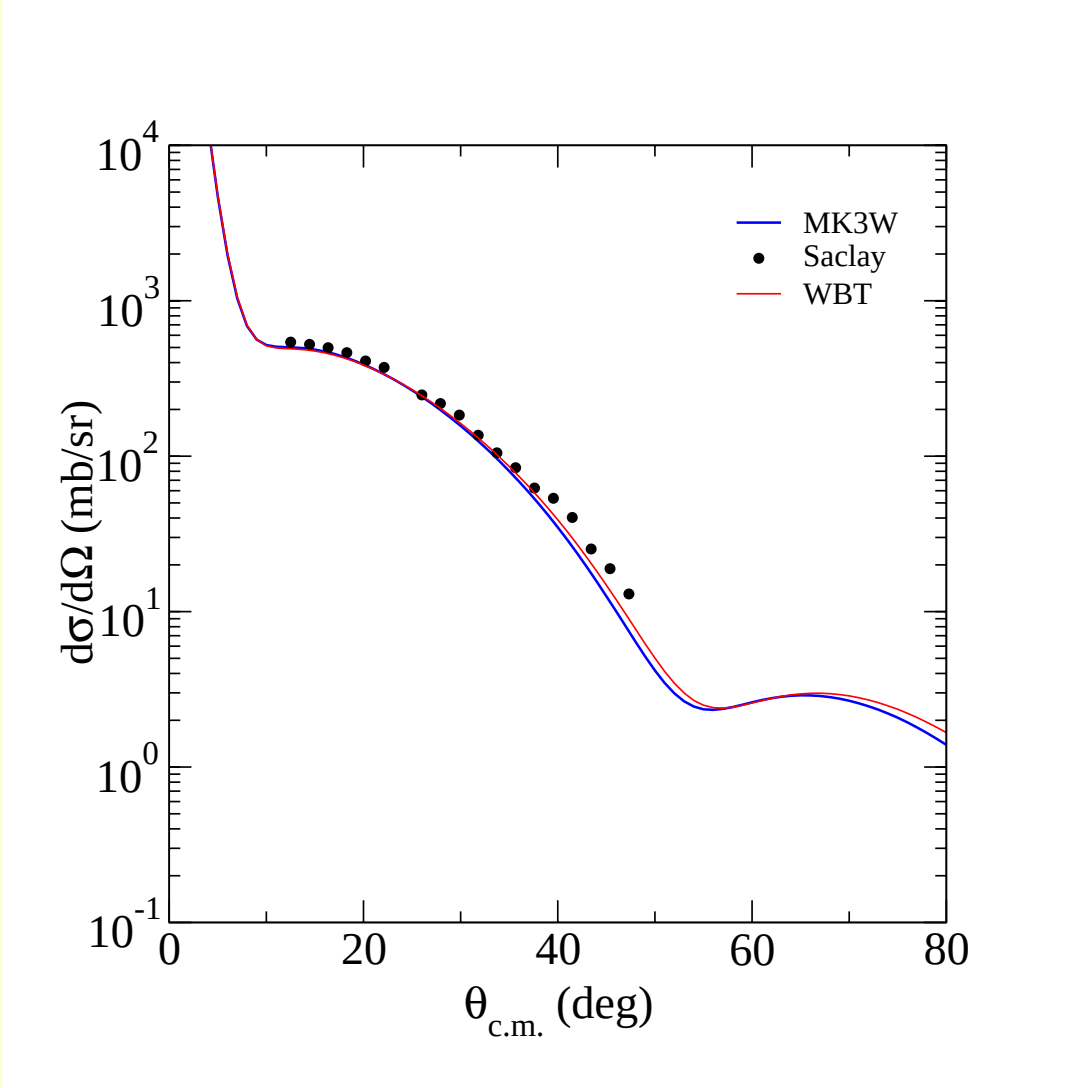

Figure 18: 45 MeV elastic proton scattering from ^{10}C.

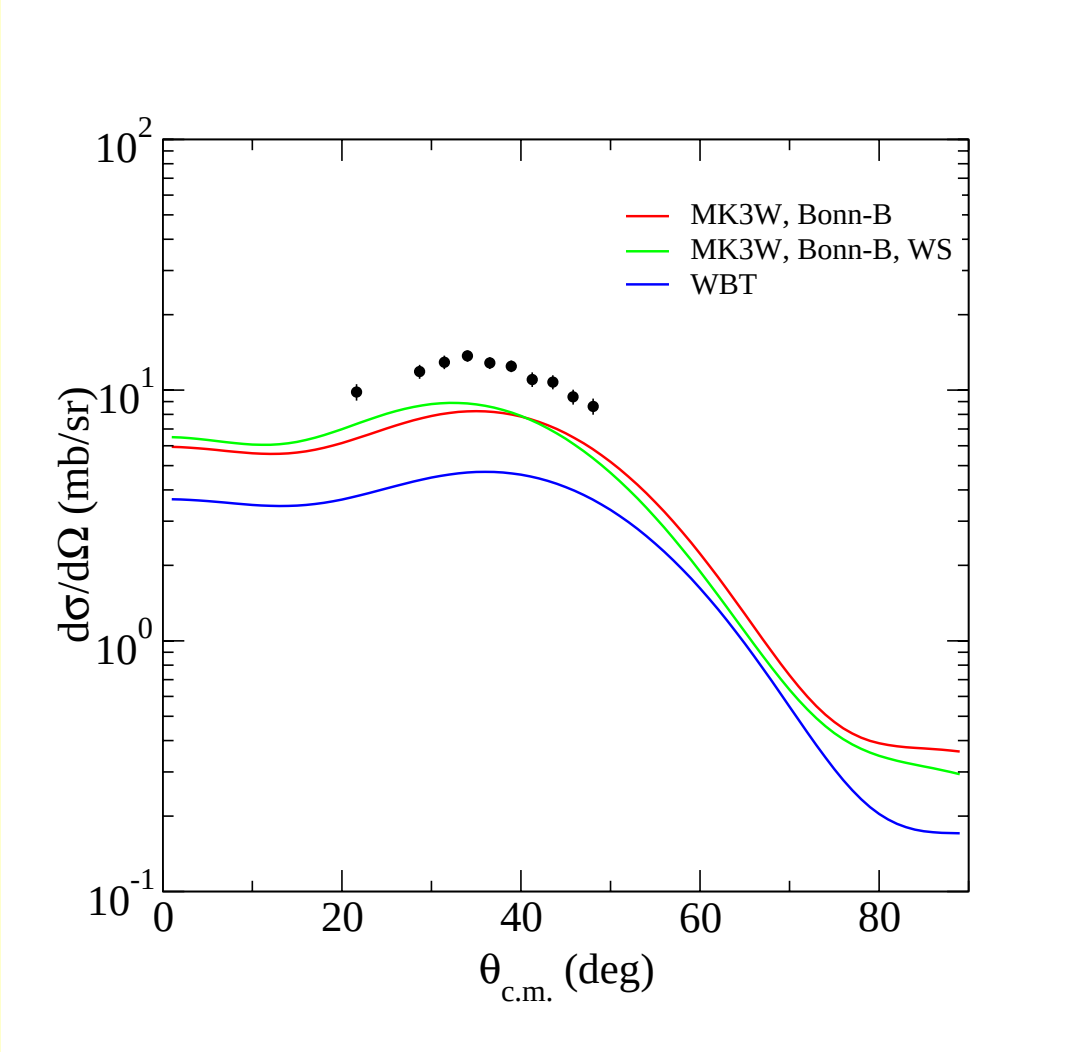

Figure 19: 45 MeV inelastic scattering from ^{10}C to the $2^+; 1$ (3.35 MeV) state.

Summary and Conclusions

- Presented a fully microscopic model of NA scattering based on effective g matrix interactions.
- Nuclear structure is essential to the model.
- Success in predicting elastic scattering cross sections, spin observables and integral observables across the mass range. This is important in applications when no measurements are available, which is especially true for neutron scattering observables.
- Using both proton and neutron scattering, we are able to obtain direct information on the neutron density in nuclei. Where proton scattering data are available, we are able to identify halos in exotic nuclei. **Scattering information is crucial in studying microscopically the wave functions of exotic nuclei.**